IEEE Access
Multidisciplinary | Rapid Review | Open Access Journal

Received October 12, 2017, accepted November 7, 2017, date of publication November 16, 2017,
date of current version December 22, 2017.

Digital Object Identifier 10.1109/ACCESS.2017.2774247

Polarized MIMO Slotted ALOHA Random Access Scheme in Satellite Network

JIALING BAI AND GUANGLIANG REN, (Member, IEEE)
The State Key Laboratory of Integrated Service Networks, Xidian University, Xi'an 710071, China

Corresponding author: Guangliang Ren (e-mail: glren@mail.xidian.edu.cn)

This work was supported in part by the National Natural Science Foundation of China under Grant 91538105 and in part by the National Basic Research Program of China (973 Program) under Grant 2014CB340206.

ABSTRACT The massive number of the machine type communication terminals accessing the satellite network brings a new challenge for the random access (RA) system. To meet the challenge, by using the polarization transmission structure in the satellite uplink, we propose a new RA scheme dubbed polarized multiple input multiple output slotted ALOHA (PMSA). In PMSA, in one slot, one packet and two overlapped packets can be decoded successfully with the polarized MIMO detection algorithms, and some of three overlapped packets may be decoded successfully in consideration of the capture effect at the satellite node. For the new features of the proposed scheme in physical layer, the protocol of medium access control (MAC) is modified based on the slotted ALOHA (SA). Simulation results show that the normalized throughput of the PMSA can reach 0.84 and is consistent with the theoretical throughput. Moreover, it is also shown that the throughput of PMSA is about 2.3 times as large as that of the SA and 1.5 times as large as that of the contention resolution diversity slotted ALOHA (CRDSA), without the need for additional transmitted power and time slots to transmit the replicas of the packets. The received packets in the proposed PMSA are processed slot by slot, not as that processed frame by frame in the CRDSA with a large additional frame delay.

INDEX TERMS MTC terminals, polarized MIMO, satellite network, slotted ALOHA, throughput.

I. INTRODUCTION

Random Access (RA) is most suitable for the massive number of machine type communication (MTC) terminals accessing the shared common channels in the satellite network among the FDMA, MF-TDMA, DAMA, and other conventional access schemes, due to the large propagation latency and the bursty traffic with a very low duty cycle in application scenarios of security, tracking, monitoring, etc.. The massive number of the MTC terminals brings a new challenge for the RA, which requires the reliable, highly spectral, low latency, large capacity and energy efficient new RA schemes to satisfy the massive terminals accessing the network with the limited bandwidth.

Many RA and their improved schemes have been investigated for the MTC terminals with the bursty traffic for many years. The well-known and widely used in the wireless network protocol is Slotted ALOHA (SA) which was first proposed by Roberts [1] and doubles the maximum throughput compared with the pure ALOHA [2]. To further improve the throughput, literature [3] proposed the Diversity Slotted ALOHA (DSA) in 1983, which specifies that the user transmits multiple copies of the same packet on different slots whenever it generates a packet. The DSA performs slightly better than the SA in terms of throughput and delay. However, due to the destructive packets collisions, both SA and DSA perform poorly over the satellite return link. In 2007, the Contention Resolution Diversity Slotted Aloha (CRDSA) [4] was introduced as an enhanced random access scheme to reduce the impact of collisions. In this scheme, each packet is sent twice in different slots randomly over a medium access control (MAC) frame and the burst collisions are processed with the iterative interference cancellation. By this way, CRDSA allows to achieve a higher normalized throughput up to 0.52 than the DSA. Afterwards, literature [5] presented another variant of CRDSA named CRDSA++ in 2009, where the same concept is extended to more than two replicas per packet (from 3 to 5 replicas). With a powerful forward error correcting (FEC) code, the maximum throughput of CRDSA-3 is equal to 0.7. The irregular repetition slotted ALOHA (IRSA) [6] is similar to the CRDSA in principle, the difference is that terminals in IRSA can transmit an irregular number of replicas over a frame, and if the optimal probability

is considered, the maximum normalized throughput obtained with IRSA can reach 0.8. Literature [7] proposed the Coded Slotted ALOHA (CSA), which is a further generalization of IRSA. In the CSA, each packet is divided into segments and then these segments are encoded via packet-oriented generic linear block codes. After that, they will be transmitted on the randomly chosen timeslots of the frame. At the receiver, with the erasure correcting codes and interference subtraction combined to resolve collisions, the maximum throughput can reach slightly above 0.8.

In summary, all the above RA schemes are designed to enhance RA performance in satellite network. The main idea of DSA, CRDSA, CRDSA++, and IRSA is to send regular or irregular replicas of the packet, and the idea of CSA is to send several encoded fragments of splitting packets at the transmitter. At the receiver side, all these RA schemes make use of the iterative interference cancellation to decode the signals. Despite the gains are obtained in the throughput by the improvement schemes, there are still some problems with these schemes in the practical applications. First, the energy efficiency is low, for one packet, the user terminal transmits many replicas on different slots in the frame, and the energy consumption of the terminal by the enhancement schemes is several times than that by the SA, which greatly degrades the lifetime of the battery-driven MTC devices [8]. Second, the gain in the throughput depends heavily on the large size of frame with several hundred of slots, and the large frame introduces an additional large latency except the propagation delay in the satellite channel. Third, in the future applications, as the number of MTC terminals increases, the channel load will be highly overloaded, and the throughputs of the available RA schemes are too low, thus it is required that the new RA scheme has a larger throughput. In the above RA schemes, it is also found that some characteristics of the satellite channel, such as the polarization characteristic, are not considered. The polarization characteristic provides an additional freedom for the packet transmission in the satellite channel, and the application of the new feature in the physical layer will further improve the performance of the RA scheme.

To improve the performance of the SA scheme, we first model the multi-user random access system as the polarized multiple input multiple output (P-MIMO) system, by using the polarization characteristic of the satellite channel. At the same time, we present the method to solve the problem of packet collisions and decode the packets with the P-MIMO. The proposed scheme makes full use of the polarization characteristic of the satellite channel to enlarge the accessing capacity of the terminals without increasing extra power and bandwidth. We dub this scheme as the PMSA. In this scheme, the user terminal does not need to transmit the replicas of the packet, since the packets can be processed within a slot, not a frame with several hundred of slots. Moreover, the energy efficiency is improved, and the additional delay is greatly decreased.

The rest of this paper is organized as follows: In Section II, system assumptions are explained. The frame structure and signal transmission model are provided in Section III. The PMSA random access scheme is proposed in Section IV. Numerical results on the physical layer and the MAC layer of PMSA are given in Section V. Finally, in Section VI, the conclusions are given.

II. SYSTEM ASSUMPTIONS

A satellite internet of things system is considered, in which a large number of MTC terminals access the satellite network through a shared RA channel, the configuration is shown in Fig.1. It is assumed that each MTC terminal is equipped with a linear cross polarization (LP) antenna, as that in literature [9], and the active terminals send the bursty packets to the satellite nodes with two polarized electromagnetic waves. At the satellite node, the horizontal and vertical polarization antennas are used to receive the vertical-polarization (VP) and the horizontal-polarization (HP) signals from terminals respectively, and the received signals are sent to the hub station at the ground. The hub station decodes the data from the received packets, and broadcasts the successfully received information to the terminals through the satellite nodes. When the received packets are not successfully decoded, the hub station also broadcasts the information to the terminals through the satellite nodes in the satellite network and the terminals will retransmit the failed packet to the satellite nodes.

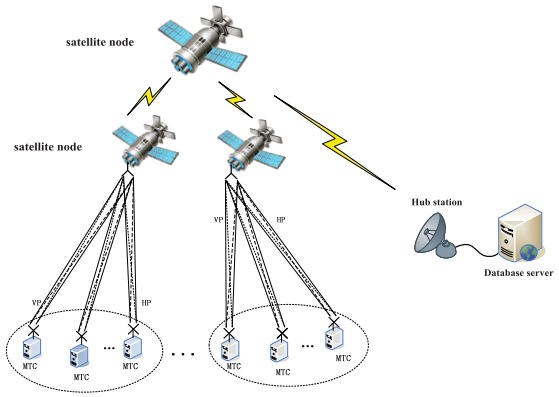

FIGURE 1. Configuration of satellite network.

For the MTC terminals, the single-carrier interleaved frequency division multiple access (SC-IFDMA) signal is employed to carry the data, as depicted in literature [10]. The various MTC terminals share the same bandwidth resource, synchronize with the broadcasting signal, and send the packets to the satellite nodes with the timing advance [11] when they generate the packets, thus the transmitted packets from different terminals arrive at the satellite nodes simultaneously.

III. POLARIZATION MIMO RANDOM ACCESS SYSTEM MODEL

In the RA system, U MTC terminals are considered, the SA protocol is modified and adjusted, and the SC-IFDMA [12] signal with low peak-to-average power ratio (PAPR) is used

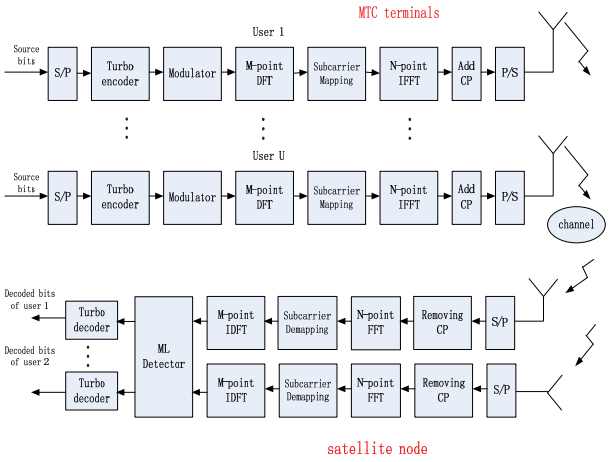

FIGURE 2. Block diagram of SC-IFDMA system.

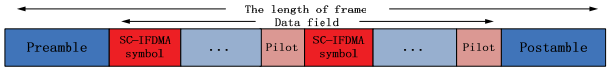

FIGURE 3. Structure of data packet.

to transmit the data packets from the MTC terminals. The schematic diagram of the SC-IFDMA based multiuser random access system is shown in Fig.2. With the SC-IFDMA signal, the terminal transmits the data in the form of packet, whose structure is the same as that in the return link of DVB-RCS2 system [13]. The structure of the packet is depicted as Fig.3. Each frame contains ξ_{pre}^{RA} preamble symbols, ξ_{pay}^{RA} payload symbols, ξ_{pos}^{RA} postamble symbols, and ξ_{pilot}^{RA} pilot symbols respectively. In addition, the pilot symbols are uniformly inserted in data symbols. The number of SC-IFDMA symbols in a data packet is $\xi_{slot}^{RA} = \xi_{pre}^{RA} + \xi_{pos}^{RA} + \xi_{pilot}^{RA} + \xi_{pay}^{RA}$. Considering that the generic bursty packets $\Gamma_{slot}^{(u)}$ generated by u^{th} MTC terminal, it can be denoted as

$$\begin{aligned}\Gamma_{slot}^{(u)} &= [\underbrace{Pre(1), \ldots, Pre(\xi_{pre}^{RA})}_{preamble}, \\ &\underbrace{\mathbf{x}_i^{(u)}(1), \ldots, \underbrace{Pilot(1), \ldots, Pilot(\xi_{pilot}^{RA})}_{pilot}, \ldots, \mathbf{x}_i^{(u)}(\xi_{pay}^{RA})}_{payload}, \\ &\underbrace{Pos(1), \ldots, Pos(\xi_{pos}^{RA})}_{postamble}] \end{aligned} \quad (1)$$

The preamble, postamble and pilots symbols are known at the receiver, and the known symbols are usually generated by the zadoff-chu (ZC) sequences for its good autocorrelation and cross correlation properties. Different terminals accessing the shared RA channel randomly select the sequences in the set of the training sequences. Once the active terminals have selected their preamble sequences in the preamble set, the corresponding pilot sequences are selected at the same time. These known symbols at the receiver are used to accomplish channel estimation, frequency offset and phase offset estimation.

For the u^{th} active terminal, the m^{th} complex SC-IFDMA symbol in the i^{th} slot can be denoted as $\mathbf{s}_i^{(u)}(m) = [s_i^{(u)}(m, 0), \ldots, s_i^{(u)}(m, M-1)]$, where M is the number of the modulated data of the m^{th} SC-IFDMA symbol in the time domain. Then after an M point discrete Fourier transform (DFT), the complex signal vector in the frequency domain can be expressed as

$$\mathbf{S}_i^{(u)}(m) = F_M \cdot \mathbf{s}_i^{(u)}(m) \quad (2)$$

where $\mathbf{S}_i^{(u)}(m) = [S_i^{(u)}(m, 0), \ldots, S_i^{(u)}(m, M-1)]$, F_M is the DFT matrix with the dimension of $M \times M$, in which the element in R^{th} row and T^{th} column is $[F_M]_{RT} = \frac{1}{\sqrt{M}} \exp(-j2\pi \cdot RT/M)$. Interleaved subcarrier mapping mode is adopted for the complex signal vector $\mathbf{S}_i^{(u)}(m)$ with low PAPR, and the occupied subcarriers are uniformly distributed over the N available subcarriers, where $N = Q \cdot M$, and Q is the spreading factor. The mapped signals $\mathbf{X}_i^{(u)}(m) = [X_i^{(u)}(m, 0), \ldots, X_i^{(u)}(m, N-1)]$ can be written as

$$X_i^{(u)}(m, l) = \begin{cases} S_i^{(u)}(m, k), & l = Q \cdot k \\ 0, & otherwise \end{cases} \quad (3)$$

where l is the index of the subcarriers for the mapped signals $\mathbf{X}_i^{(u)}(m)$, and $0 \le l \le N-1$, k is the index of the subcarrier for the m^{th} SC-IFDMA symbol in the frequency domain and $0 \le k \le M-1$. After the subcarrier mapping, an N point inverse FFT (IFFT) is employed to generate the complex signal in time domain as follows:

$$\mathbf{x}'^{(u)}_i(m) = F_N \cdot \mathbf{X}_i^{(u)}(m) \quad (4)$$

where $\mathbf{x}'^{(u)}_i(m) = [x_i^{(u)}(m, 0), \ldots, x_i^{(u)}(m, N-1)]$, F_N is the $N \times N$ IFFT matrix whose $(J, K)^{th}$ element is $[F_N]_{JK} = \frac{1}{\sqrt{N}} \exp(j2\pi \cdot JK/N)$. At last, cyclic prefix (CP) is inserted into the signal sequence, then the transmitted complex baseband signal can be described as

$$\begin{aligned}\mathbf{x}_i^{(u)}(m) = [&x_i^{(u)}(m, N-L_{cp}), \ldots, x_i^{(u)}(m, N-1), \\ &x_i^{(u)}(m, 0), \ldots, x_i^{(u)}(m, N-1)]^T \end{aligned} \quad (5)$$

where $\{\cdot\}^T$ denotes the transpose of $\{\cdot\}$. L_{cp} is the length of CP and the length of m^{th} SC-IFDMA symbol is $N + L_{cp}$. In the RF modulator, the complex baseband signal is converted to the pass-band signal, and transmitted by the cross linear polarization antenna equipped at the MTC terminals.

The cross linear polarization antenna of the MTC terminal transmits two polarized electromagnetic waves, and two polarized antennas are employed to receive the two different polarized electromagnetic waves respectively at the satellite node. The channel between the u^{th} active terminal and the satellite node is the 2×2 polarized MIMO channel, and its complex baseband presentation during the m^{th} symbol on the

i^{th} slot can be described as

$$\mathbf{h}_i^{(u)}(m) = \begin{bmatrix} \mathbf{h}_{i,VV}^{(u)}(m) & \mathbf{h}_{i,VH}^{(u)}(m) \\ \mathbf{h}_{i,HV}^{(u)}(m) & \mathbf{h}_{i,HH}^{(u)}(m) \end{bmatrix} \tag{6}$$

where $\mathbf{h}_{i,VV}^{(u)}(m)$ and $\mathbf{h}_{i,HH}^{(u)}(m)$ represent the co-polarization channel impulse responses between the VP/HP transmitter and VP/HP receiver respectively, $\mathbf{h}_{i,HV}^{(u)}(m)$ and $\mathbf{h}_{i,VH}^{(u)}(m)$ are the cross-polarization channel impulse responses between the VP/HP transmitter and HP/VP receiver respectively.

The received signal vector of the u^{th} active terminal can be denoted as $\mathbf{y}_i^{(u)}(m) = [\mathbf{y}_{i,V}^{(u)}(m), \mathbf{y}_{i,H}^{(u)}(m)]^T$, where $\mathbf{y}_{i,V}^{(u)}(m)$ and $\mathbf{y}_{i,H}^{(u)}(m)$ are the complex signals received by the VP antenna and the HP antenna respectively. During the m^{th} symbol on the i^{th} slot, the received signal vector of the u^{th} active terminal at the receiver in the satellite node can be represented as

$$\begin{aligned} \mathbf{y}_i^{(u)}(m) &= \begin{bmatrix} \mathbf{y}_{i,V}^{(u)}(m) \\ \mathbf{y}_{i,H}^{(u)}(m) \end{bmatrix} \\ &= \begin{bmatrix} \mathbf{h}_{i,VV}^{(u)}(m) & \mathbf{h}_{i,VH}^{(u)}(m) \\ \mathbf{h}_{i,HV}^{(u)}(m) & \mathbf{h}_{i,HH}^{(u)}(m) \end{bmatrix} \begin{bmatrix} \mathbf{x}_i^{(u)}(m) \\ \mathbf{x}_i^{(u)}(m) \end{bmatrix} + \begin{bmatrix} \mathbf{n}_{i,V}(m) \\ \mathbf{n}_{i,H}(m) \end{bmatrix} \\ &= \begin{bmatrix} \left[\mathbf{h}_{i,VV}^{(u)}(m) + \mathbf{h}_{i,VH}^{(u)}(m)\right] \mathbf{x}_i^{(u)}(m) \\ \left[\mathbf{h}_{i,HV}^{(u)}(m) + \mathbf{h}_{i,HH}^{(u)}(m)\right] \mathbf{x}_i^{(u)}(m) \end{bmatrix} + \begin{bmatrix} \mathbf{n}_{i,V}(m) \\ \mathbf{n}_{i,H}(m) \end{bmatrix} \\ &= \begin{bmatrix} \mathbf{h}_{i,V}^{(u)}(m)\mathbf{x}_i^{(u)}(m) \\ \mathbf{h}_{i,H}^{(u)}(m)\mathbf{x}_i^{(u)}(m) \end{bmatrix} + \begin{bmatrix} \mathbf{n}_{i,V}(m) \\ \mathbf{n}_{i,H}(m) \end{bmatrix} \end{aligned} \tag{7}$$

where

$$\mathbf{h}_{i,V}^{(u)}(m) = \mathbf{h}_{i,VV}^{(u)}(m) + \mathbf{h}_{i,VH}^{(u)}(m) \tag{8}$$

$$\mathbf{h}_{i,H}^{(u)}(m) = \mathbf{h}_{i,HH}^{(u)}(m) + \mathbf{h}_{i,HV}^{(u)}(m). \tag{9}$$

$\mathbf{h}_{i,pq}^{(u)}(m)(p, q \in \{VorH\})$ is independent with each other, and $\mathbf{n}_{i,V}(m)$ and $\mathbf{n}_{i,H}(m)$ are the complex additive white Gaussian noise vector respectively.

For the given slot in the shared RA satellite channel, it is assumed that $L(0 \leq L \leq U)$ active terminals transmit the packets simultaneously. The received signals from two polarization antennas at the receiver in the satellite node can be expressed as

$$\mathbf{y}_i(m) = \sum_{u=1}^{L} \mathbf{y}_i^{(u)}(m) + \mathbf{n}_i(m) \tag{10}$$

where $\mathbf{y}_i(m) = [\mathbf{y}_{i,V}(m), \mathbf{y}_{i,H}(m)]^T$. The received signal vector can be further described as follows:

$$\begin{aligned} \mathbf{y}_i(m) &= \begin{bmatrix} \mathbf{y}_{i,V}(m) \\ \mathbf{y}_{i,H}(m) \end{bmatrix} \\ &= \begin{bmatrix} \sum_{u=1}^{L} \mathbf{y}_{i,V}^{(u)}(m) \\ \sum_{u=1}^{L} \mathbf{y}_{i,H}^{(u)}(m) \end{bmatrix} + \begin{bmatrix} \mathbf{n}_{i,V}(m) \\ \mathbf{n}_{i,H}(m) \end{bmatrix} \\ &= \begin{bmatrix} \sum_{u=1}^{L} \mathbf{h}_{i,V}^{(u)}(m)\mathbf{x}_i^{(u)}(m) \\ \sum_{u=1}^{L} \mathbf{h}_{i,H}^{(u)}(m)\mathbf{x}_i^{(u)}(m) \end{bmatrix} + \begin{bmatrix} \mathbf{n}_{i,V}(m) \\ \mathbf{n}_{i,H}(m) \end{bmatrix} \\ &= \begin{bmatrix} \mathbf{h}_{i,V}^{(1)}(m) & \mathbf{h}_{i,V}^{(2)}(m) & \cdots & \mathbf{h}_{i,V}^{(L)}(m) \\ \mathbf{h}_{i,H}^{(1)}(m) & \mathbf{h}_{i,H}^{(2)}(m) & \cdots & \mathbf{h}_{i,H}^{(L)}(m) \end{bmatrix} \\ &\quad \cdot \begin{bmatrix} \mathbf{x}_i^{(1)}(m) \\ \mathbf{x}_i^{(2)}(m) \\ \vdots \\ \mathbf{x}_i^{(L)}(m) \end{bmatrix} + \begin{bmatrix} \mathbf{n}_{i,V}(m) \\ \mathbf{n}_{i,H}(m) \end{bmatrix}. \end{aligned} \tag{11}$$

Equation (11) shows that the model of the multiuser signals transmission in the RA system is the $L \times 2$ MIMO transmission model, and the MIMO detection scheme [14], [15] can be used to decode the received signals.

IV. PROPOSED RANDOM ACCESS SCHEME

The polarized MIMO transmission provides the additional freedom for the hub station to resolve the collision packets. With the new transmission structure in the RA, the processing and controlling protocol are different with that in the conventional SA. This new RA scheme is dubbed as PMSA. In this section, the detail of the PMSA scheme and the theoretical throughput is presented.

A. PMSA

In the PMSA scheme, the MTC terminals synchronize to the satellite node by using the broadcasting messages in the downlink, and send the packets with the cross polarized antennas when they are active. The satellite node receives two polarized signals respectively. The timing advance (TA) technique [11] is employed by the activated MTC terminals, thus the transmitted packets from different terminals arrive at the satellite node simultaneously. Due to the uncoordinated terminals, the cases of the overlapped packets in the two received polarized antennas in one slot are shown in Fig.4. It can be seen that there are five cases in each slot at the satellite node, which is given as follows.

1) CASE 1

There is not a packet transmitted in a given slot on the two antennas.

2) CASE 2

There is only one packet transmitted in a given slot on the two antennas.

3) CASE 3

There are two packets transmitted in a given slot on the two antennas.

4) CASE 4

There are three packets transmitted in a given slot on the two antennas.

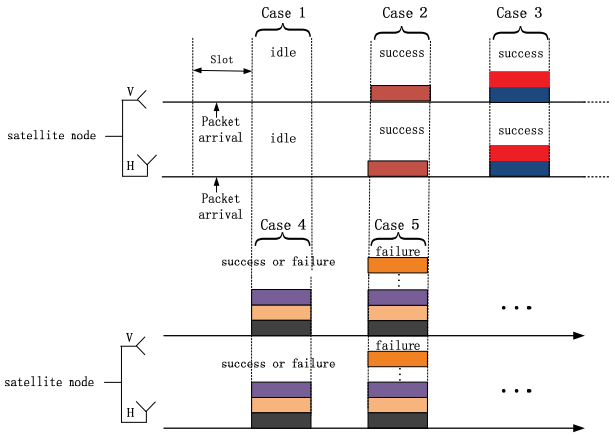

FIGURE 4. Situations of bursts transmission using PMSA.

5) CASE 5

There are more than three packets transmitted in a given slot on the two antennas.

For the case 1, the given slot is considered as idle, and no further processing is needed for the received signals in the given slot, which is the same as that in the conventional SA.

For the case 2, there is only one packet in the given slot, and two received signals of the same packet are independent due to different polarized states. By setting $L = 1$ in the (11), the received m^{th} symbol vector in the given i^{th} slot at the satellite node can be described as

$$\mathbf{y}_i(m) = \begin{bmatrix} \mathbf{y}_{i,V}(m) \\ \mathbf{y}_{i,H}(m) \end{bmatrix} = \begin{bmatrix} \sum_{u=1}^{L} \mathbf{y}_{i,V}^{(u)}(m) \\ \sum_{u=1}^{L} \mathbf{y}_{i,H}^{(u)}(m) \end{bmatrix} + \begin{bmatrix} \mathbf{n}_{i,V}(m) \\ \mathbf{n}_{i,H}(m) \end{bmatrix} = \begin{bmatrix} \mathbf{h}_{i,V}^{(1)}(m) \\ \mathbf{h}_{i,H}^{(1)}(m) \end{bmatrix} \mathbf{x}_i^{(1)}(m) + \begin{bmatrix} \mathbf{n}_{i,V}(m) \\ \mathbf{n}_{i,H}(m) \end{bmatrix}. \quad (12)$$

By using the preambles and pilots in the received packets, the channel coefficients can be estimated as $\hat{\mathbf{h}}_i^{(1)}(m) = [\hat{\mathbf{h}}_{i,V}^{(1)}(m), \hat{\mathbf{h}}_{i,H}^{(1)}(m)]^T$. For the two received signals, the maximal ratio combining (MRC) technique can be used to combine the received signals, which can be represented as

$$\hat{\mathbf{x}}_i^{(1)}(m) = \frac{\hat{\mathbf{h}}_i(m)^H \mathbf{y}_i(m)}{\hat{\mathbf{h}}_i(m)^H \hat{\mathbf{h}}_i(m)} \quad (13)$$

where $\{\cdot\}^H$ denotes the Hermitian transpose of $\{\cdot\}$. By using the combine technique for all the symbols in the packet, the combined signals can be decoded and the transmitted data is recovered finally as that in the conventional SA.

Case 3, case 4 and case 5 are the collision scenarios, which can be further processed as analyzed in the following subsection.

B. COLLISION RESOLUTION IN PMSA

For the case 3, in the conventional SA, it is regarded as the collision and the two packets will be discarded, thus the terminals will retransmit the packets without receiving the knowledge of ACKs from the satellite node. However, for the proposed PMSA, due to the new polarized MIMO transmission structure, the two overlapped packets can be recovered by the MIMO detection algorithm.

For the case 3, by setting $L = 2$ in the (11), the received m^{th} symbol vector in the given i^{th} slot at the satellite node can be described as

$$\begin{bmatrix} \mathbf{y}_{i,V}(m) \\ \mathbf{y}_{i,H}(m) \end{bmatrix} = \begin{bmatrix} \mathbf{h}_{i,V}^{(1)}(m) & \mathbf{h}_{i,V}^{(2)}(m) \\ \mathbf{h}_{i,H}^{(1)}(m) & \mathbf{h}_{i,H}^{(2)}(m) \end{bmatrix} \begin{bmatrix} \mathbf{x}_i^{(1)}(m) \\ \mathbf{x}_i^{(2)}(m) \end{bmatrix} + \begin{bmatrix} \mathbf{n}_{i,V}(m) \\ \mathbf{n}_{i,H}(m) \end{bmatrix}. \quad (14)$$

Equation (14) shows that the two signals of the two terminals and the two received signals constructs a 2×2 MIMO model, and the overlapped signals of the two terminals can be recovered by the MIMO detection algorithm.

At the satellite receiver, by using the preambles and pilots for two terminals in the received packets, one can obtain the channel coefficient matrix as

$$\tilde{\mathbf{h}}_i(m) = \begin{bmatrix} \tilde{\mathbf{h}}_{i,V}^{(1)}(m) & \tilde{\mathbf{h}}_{i,V}^{(2)}(m) \\ \tilde{\mathbf{h}}_{i,H}^{(1)}(m) & \tilde{\mathbf{h}}_{i,H}^{(2)}(m) \end{bmatrix}. \quad (15)$$

With the estimated channel matrix, the MIMO detection techniques, such as maximum likelihood (ML) equalization, will be used to detect the signals from two different MTC terminals. By calculating the Euclidean distance between the received signal vector and all the vectors in the transmitted symbols set [14], the transmitted signal vector $\mathbf{x}_i(m) = [\mathbf{x}_i^{(1)}(m), \mathbf{x}_i^{(2)}(m)]^T$ is estimated by the ML detection algorithm as follows:

$$\tilde{\mathbf{x}}_{i,ML}(m) = \arg\min_{\mathbf{x}_i(m)} ||\mathbf{y}_i(m) - \tilde{\mathbf{h}}_i(m)\mathbf{x}_i(m)||^2 \quad (16)$$

where $\mathbf{y}_i(m) = [\mathbf{y}_{i,V}(m), \mathbf{y}_{i,H}(m)]^T$. By using the ML detection algorithm for all the symbols in the packets, one can obtain all the detected symbols, and which can be decoded to recover the transmitted data in the packets. Therefore, two overlapped packets can be decoded successfully in the case 3.

For the case 4, there are overlapped packets of three terminals in one slot, by setting $L = 3$ in the (11), the received m^{th} symbol vector in the given i^{th} slot at the satellite node can be described as

$$\begin{bmatrix} \mathbf{y}_{i,V}(m) \\ \mathbf{y}_{i,H}(m) \end{bmatrix} = \begin{bmatrix} \mathbf{h}_{i,V}^{(1)}(m) & \mathbf{h}_{i,V}^{(2)}(m) & \mathbf{h}_{i,V}^{(3)}(m) \\ \mathbf{h}_{i,H}^{(1)}(m) & \mathbf{h}_{i,H}^{(2)}(m) & \mathbf{h}_{i,H}^{(3)}(m) \end{bmatrix} \cdot \begin{bmatrix} \mathbf{x}_i^{(1)}(m) \\ \mathbf{x}_i^{(2)}(m) \\ \mathbf{x}_i^{(3)}(m) \end{bmatrix} + \begin{bmatrix} \mathbf{n}_{i,V}(m) \\ \mathbf{n}_{i,H}(m) \end{bmatrix}. \quad (17)$$

It can be seen that the solution of the (17) is not unique when three packet signals have the same power. Thus the transmitted symbols of the three terminals cannot be detected by the MIMO detection algorithms, all of the packets will be lost, which is also true for the case 5. However, for the case

4, if the capture effect is considered, the overlapped packets of three users may be recovered in the PMSA.

For the case of three packets overlapped, if the SINR of the packet with the strongest power is greater than the threshold of the capture effect, the packet can be processed and decoded as that in case 2, then one can reconstruct the received packet signals on two antennas with the decoded bits, and subtract the reconstructed signals from the overlapped packet signals on the two antennas. The remained signals are the same as those in case 3, the MIMO detection algorithm can be used to process and decode the two packets. The detail is given as follows.

Three bursty packets from three users can be expressed as $\mathbf{x}_i^{(u)}$, $(u = 1, 2, 3)$, $\mathbf{x}_i^{(2)}$ and $\mathbf{x}_i^{(3)}$ have the same power, whereas the power of user $\mathbf{x}_i^{(1)}$ is higher than $\mathbf{x}_i^{(2)}$ and $\mathbf{x}_i^{(3)}$, and its SINR is greater than the threshold of the capture effect. The received signals in (17) can be rewritten as

$$\begin{aligned}\underbrace{\begin{bmatrix}\mathbf{y}_{i,V}(m)\\ \mathbf{y}_{i,H}(m)\end{bmatrix}}_{\mathbf{y}} &= \underbrace{\begin{bmatrix}\mathbf{h}_{i,V}^{(1)}(m)\\ \mathbf{h}_{i,H}^{(1)}(m)\end{bmatrix}\begin{bmatrix}\mathbf{x}_i^{(1)}(m)\end{bmatrix}}_{\mathbf{y}_1}\\ &+ \underbrace{\begin{bmatrix}\mathbf{h}_{i,V}^{(2)}(m) & \mathbf{h}_{i,V}^{(3)}(m)\\ \mathbf{h}_{i,H}^{(2)}(m) & \mathbf{h}_{i,H}^{(3)}(m)\end{bmatrix}\begin{bmatrix}\mathbf{x}_i^{(2)}(m)\\ \mathbf{x}_i^{(3)}(m)\end{bmatrix}}_{\mathbf{y}_2}\\ &+ \begin{bmatrix}\mathbf{n}_{i,V}(m)\\ \mathbf{n}_{i,H}(m)\end{bmatrix} \qquad (18)\end{aligned}$$

where $\mathbf{y_1}$ and $\mathbf{y_2}$ are the strongest signal and two weak signals received from two polarized antennas respectively. It can be found that $\mathbf{y_1}$ is the main part of the received signals. In order to decode the strongest signal firstly, the weak received signals $\mathbf{y_2}$ can be seen as the interference. By using the same process as that in case 2, the combined signal for the first user $\mathbf{x}_i^{(1)}(m)$ is obtained as

$$\widehat{\mathbf{x}}_i^{(1)}(m) = \frac{\widehat{\mathbf{h}}_i^{(1)}(m)^H \mathbf{y}_i(m)}{\widehat{\mathbf{h}}_i^{(1)}(m)^H \widehat{\mathbf{h}}_i^{(1)}(m)} \qquad (19)$$

where $\widehat{\mathbf{h}}_i^{(1)}(m) = [\widehat{\mathbf{h}}_{i,V}^{(1)}(m), \widehat{\mathbf{h}}_{i,H}^{(1)}(m)]^T$ is the estimated channel coefficients for $\mathbf{x}_i^{(1)}(m)$. By using the same operation for all the symbols, the combined signal can be decoded. With the decoded bits of the packet and the channel coefficients, the received strongest signal can be reconstructed as $\mathbf{y'}_1 = \widehat{\mathbf{h}}_i^{(1)}(m)\breve{\mathbf{x}}_i^{(1)}(m)$, $\breve{\mathbf{x}}_i^{(1)}(m)$ is the reconstructed strong signal. By cancelling the reconstructed signal from the received signals $\mathbf{y}$, we can get the sum of two weak signals as follows:

$$\mathbf{y'}_2 = \mathbf{y} - \mathbf{y'}_1 \qquad (20)$$

where $\mathbf{y'}_2$ expresses the remained component after the interference cancellation. With the estimated channel coefficients $\widehat{\mathbf{h}}_i'(m) = \begin{bmatrix}\widehat{\mathbf{h}}_{i,V}^{(2)}(m) & \widehat{\mathbf{h}}_{i,V}^{(3)}(m)\\ \widehat{\mathbf{h}}_{i,H}^{(2)}(m) & \widehat{\mathbf{h}}_{i,H}^{(3)}(m)\end{bmatrix}$, two weak signals can be detected as that in case 3. Therefore, three unequal-power packets may be decoded successfully in case 4.

C. THEORETICAL THROUGHPUT OF PMSA

Different with the SA, PMSA can decode one packet and two overlapped packets in one slot, due to the polarized MIMO transmission structure. Consider that the same condition as that in the theoretical throughput derivation of the SA, the theoretical throughput of the PMSA can be derived as follows.

In the MTC communication systems, Poisson distribution is one of the mathematical models to describe the random access behavior for MTC scenario [16]–[19]. Since there is infinite user population in M2M network, the number of the generation of packets is assumed to follow a Poisson distribution, and the probability to generate n packets in the period t is given as

$$p_n(t) = \frac{e^{-\lambda t}(\lambda t)^n}{n!} \qquad (21)$$

where λ is the expected number of packets to generate in a unit time. If the duration of a packet is defined as τ and the duration of the slot has the same value as the packet. The traffic G is given as

$$G = \lambda\tau. \qquad (22)$$

Here, we assume that the retransmission time is randomized enough, thus the arrival process of retransmission packets can be regarded as the Poisson process too. From the above sub-sections, it can be seen that the packets will be successfully transmitted from the terminals to the satellite node only in case 2 and case 3. For all the uncoordinated terminals, the successful transmission probability can be given as

$$\begin{aligned}P_{succ} &= P_0 + P_1\\ &= \frac{e^{-\lambda\tau}(\lambda\tau)^0}{0!} + \frac{e^{-\lambda\tau}(\lambda\tau)^1}{1!}\\ &= e^{-G} + Ge^{-G}. \qquad (23)\end{aligned}$$

Therefore, the theoretical throughput of the PMSA can be represented as

$$S = GP_{succ} = G(1+G)e^{-G}. \qquad (24)$$

By taking the derivative of the (24) with respect to G, and setting the derivation to be zero, one can get

$$\frac{\partial S}{\partial G} = (1 + G - G^2)e^{-G} = 0. \qquad (25)$$

It is easy to find that the maximum throughput of the PMSA is about 0.84, and its corresponding normalized load is $G = \frac{1+\sqrt{5}}{2} \approx 1.62$, which is also the critical point of the PMSA.

D. STABILITY ANALYSIS IN PMSA

The transmission mechanism of the proposed scheme is similar to that of the SA because they both transmit packets slot by slot, and once the number of arriving packets exceeds the system processing capability, the packets will be lost. Therefore, the stability analysis of the proposed technique is also similar to that of SA [20]–[22] with the Markovian model. It is assumed that the satellite channel with a user population consisting of M users (finite or infinite), each user can be in one of two states: Thinking (T) or Backlogged (B). In the thinking state, a user generates and transmits a new packet in a time slot with probability σ. Each backlogged retransmits in the current time slot with probability p, and the total number of backlogged packets at the current slot is n_b. The expected channel input in the current slot is S_T and the expected total channel load is S_{total}, thus we have $S_{total} = S_T + n_b$. The expected channel load is equal to the expected throughput. Thus, according to [20], [21]

$$S_T = S_{total}(1 - PLR) \tag{26}$$

$$n_b = n_b(1 - p) + S_{total}PLR \tag{27}$$

from which

$$n_b = \frac{S_{total}PLR}{p}. \tag{28}$$

Moreover, the expected channel input can be entirely described by the so called channel load line, which represents the relation between the S_T and the number of backlogged packets n_b for satellite scenario. The channel load line can be defined as

$$S_T = (M - n_b)\sigma \tag{29}$$

So the equilibrium contours is given in Fig.5.

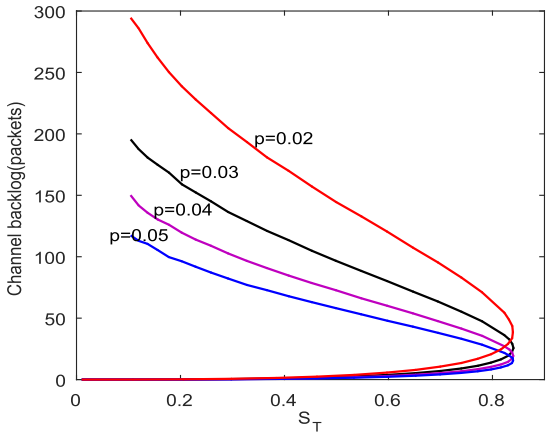

FIGURE 5. Equilibrium contours in the (n_b, S_T) plane.

According to the conclusions from [20] and [21], if the channel load line intersects the equilibrium contour in exactly one place, then it said to be stable. When the M is finite, a stable channel can always be achieved. For example, suppose the same retransmission probability with SA of $p = 0.02$ and user population of $M = 200$, when $\sigma = 1/243.9$, the equilibrium channel throughput rate at the channel operating point is $S_o = 0.78$, the average backlog time D_b is about 26 slots, whereas for the SA, the $S_o = 0.346$ and D_b is about 58 slots when the $\sigma = 1/536.1$. Obviously, the proposed scheme has a better stability performance than SA. A detailed similar discussion of the various circumstances is given in [20] and [21]. Thus in order to provide an efficient communication, the key issue is to find the tradeoff between stability, throughput and delay, which is based on the design of the system. If a stable channel is wanted, then one should limit its use to a small population of users and sacrificing channel utilization, on the other hand, an unstable channel could support a large population of users operating at a certain level of reliability.

V. NUMERICAL RESULTS

The performance of the proposed PMSA is investigated by the computer simulation. The packet error rate (PER), throughput, packet loss rate (PLR) and the energy efficiency are given in the simulation. And the SA, CRDSA, CRDSA-3, and IRSA are also simulated to compare with the proposed scheme. Furthermore, the effects of fading and noise have been considered in discussing the PER performance for various cases (one packet, two bursty packets, and three bursty packets in current slot), and when discussing the effects of the various SNR values, capture thresholds and the energy efficiency to the throughput performance, the fading and noise is also considered. The effects of the fading contain the small scale fading and the large scale fading. The small scale fading is given in the channel model ITU-R M.1225 as in Table 1, and the large scale fading follows the log-normally distribution with 0dB mean and standard deviation $\sigma = 3dB$. The main parameters of the satellite system with the proposed RA scheme are depicted in Table.1.

TABLE 1. Simulation parameters.

Parameter	Value
Modulation scheme	BPSK
Encode type	1/2 Turbo code
Channel model	ITU-R M.1225
No. of Sub-carrier/output block size(N)	256
Message Block Size/input block size(M)	64
No. of data symbols in one packet	18
Length of packet	576 bits

A. RESULTS WITH FADING AND NOISE IN PHYSICAL LAYER

Fig.6 shows the PER performance for the case 2 and case 3 in the PMSA scheme. It can be seen that the PER is below 0.1 when the SNR is greater than 0dB for the case 2, due to the diversity of the two polarized receive antennas. For the case 3, the PER is below 0.1 when the SNR is greater than 4dB, which shows that the two overlapped packets can be effectively decoded with the polarized MIMO structure.

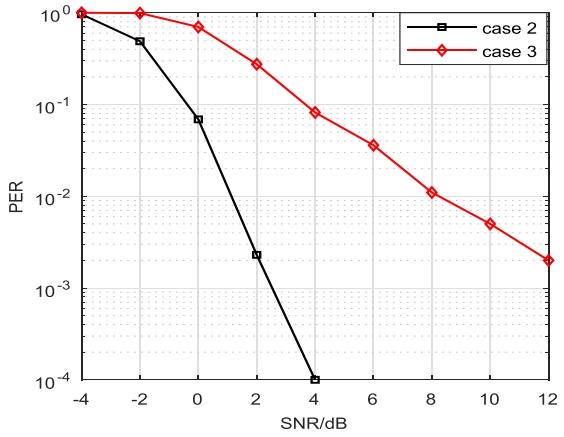

FIGURE 6. PER versus SNR for single packet and two overlapped packets.

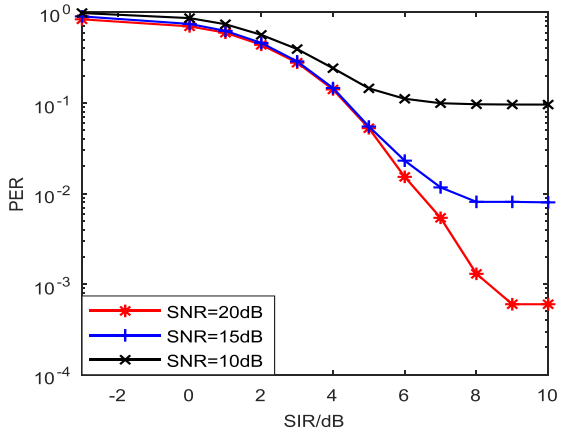

FIGURE 7. PER versus SIR for three bursty packets under different SNR (10dB, 15dB, 20dB).

Fig.7 shows PER vs. SIR for three packets under different SNR values (10dB, 15dB, 20dB) for the case 4. The SIR is defined as the strongest power signal to the sum of two weak power signals ratio. And the SNR is defined as the weak power signal to noise ratio, they are given as follows,

$$SIR = \frac{P_{strongest}}{\sum_{i=1}^{2} P_{weak,i}} \tag{30}$$

$$SNR = \frac{P_{weak}}{P_{noise}} \tag{31}$$

It can be seen from Fig.7 that the PER performance is closely related to both the interference and the noise. For a fixed SNR, when the SIR increases from −3dB to 10dB, the power difference between the strongest signal and the sum of two weak signals becomes larger, the PER performance is getting better. On the other hand, for a fixed SIR, the PER decreases as the SNR increases, particularly under high SIR value. Based on the relation between the PER and the SIR, the capture thresholds will be determined. Since the large capture threshold will result in the reduced probability of the packets satisfying the corresponding capture thresholds, the suitable capture thresholds should be set to make a compromise between the PER performance and the packets probability. Throughput of the proposed scheme versus the normalized load for different thresholds of the capture effect will be discussed later.

B. RESULTS AT HIGH SNR REGION IN MAC LAYER

Fig.8 shows the throughputs of PMSA, SA, CRDSA, CRDSA-3, and IRSA at high SNR region. It can be seen that the theoretical throughput of the PMSA is in agreement with the simulated throughput of PMSA, and the maximum throughput of the PMSA can reach 0.84 when the normalized MAC load G is 1.62. Compared the PMSA with the reference schemes, when the normalized MAC load G is smaller than 0.65, the throughput of PMSA is about the same as those of the CRDSA, CRDSA-3, and IRSA, and is larger than that of the SA. When the normalized load G is greater than 0.65 and less than 0.9, the throughput of PMSA is slightly less than the CDRSA-3 and IRSA. When the normalized load G is larger than 0.9, PMSA will show much better throughput performance and keep a steady downward trend than the others.

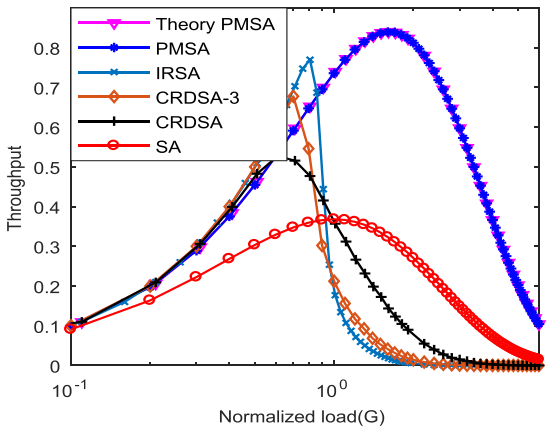

FIGURE 8. Normalized throughputs versus normalized load for PMSA, SA, CRDSA(with 2 repetitions), CRDSA-3(with 3 repetitions), and IRSA with $\Lambda_3(x) = 0.5x^2 + 0.28x^3 + 0.22x^8$.

In Fig.9, the PLRs for the PMSA and different CRDSA, IRSA schemes are compared. It can be seen that the PLR of the PMSA is much better than that of the SA, and is about the same as that of the CRDSA when G is less than 0.65. The PLR performance of the PMSA is worse than those of the CRDSA-3 and IRSA when the normalized load is below 0.9. The PLR of the PMSA is much better than those of the SA and CRDSA when G is greater than 0.65, and is better than those of the CRDSA-3 and IRSA when G is greater than 0.9. Furthermore, for the given PLR of about 10^{-2}, the channel load of the PMSA is 17 times than that of the SA.

Fig.10 shows the energy efficiency of the PMSA, SA, CRDSA, CRDSA-3, and IRSA at high SNR region. According to the literature [23], the transmission energy efficiency is given as

$$\eta = \frac{E(N_{TX}^{succ})\varepsilon_{TX}}{E(N_{TX})\varepsilon_{TX}} \tag{32}$$

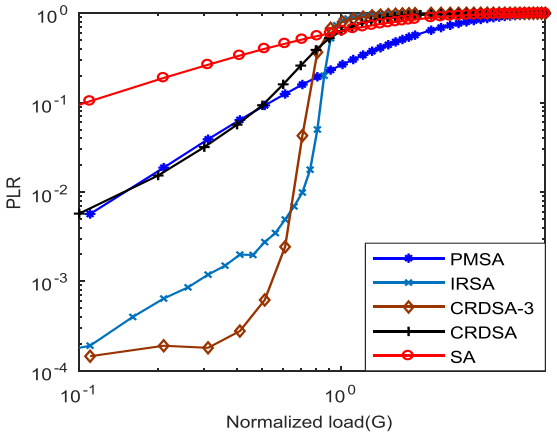

FIGURE 9. Packet loss rate versus normalized load for PMSA, SA, CRDSA(with 2 repetitions), CRDSA-3(with 3 repetitions), and IRSA with $\Lambda_3(x) = 0.5x^2 + 0.28x^3 + 0.22x^8$.

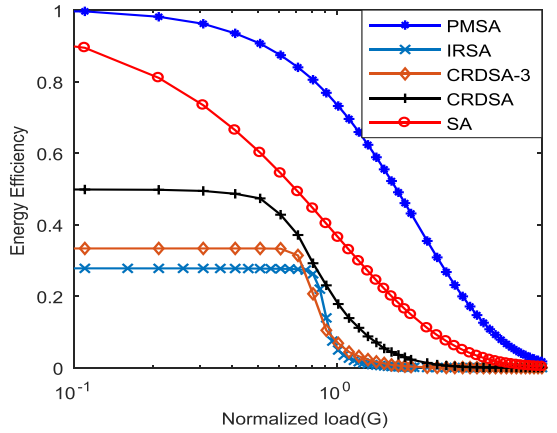

FIGURE 10. Energy efficiency versus normalized load for PMSA, SA, CRDSA(with 2 repetitions), CRDSA-3(with 3 repetitions), and IRSA with $\Lambda_3(x) = 0.5x^2 + 0.28x^3 + 0.22x^8$.

where N_{TX} denotes the total number of transmitted packets, N_{TX}^{succ} is the number of successfully received packets, and ε_{TX} is the transmission energy of a packet. It can be seen from Fig.10 that the PMSA yields a much better performance than those of the others. When the normalized load is below 0.65, the energy efficiency of the PMSA is higher than 0.9, and the CRDSA and CRDSA-3 are only about 0.5 and 0.33 respectively. IRSA is then much lower than the PMSA, which is only about 0.27, less than one-third of the PMSA. When the normalized load is over 0.9, the energy efficiency of the CRDSA, CRDSA-3, and IRSA drops sharply and approaches to zero, which is much worse than that of the PMSA. Furthermore, when the normalized load is about 2, the energy efficiency of the PMSA is still about 0.4.

C. RESULTS WITH FADING AND NOISE IN MAC LAYER

Fig.11 shows the throughputs of the PMSA versus the normalized load for different SNRs. The theoretical curve is given without considering the capture effect and the noise, whereas other simulation curves in Fig.11 have taken into account the effects of noise. It can be seen that the throughput of PMSA approaches to the theoretical throughput as the SNR increases. When the SNR is greater than 9dB, the throughput of the PMSA is about the same as the theoretical throughput. As the SNR decreases, the throughput of the PMSA decreases, due to the errors introduced by the noise.

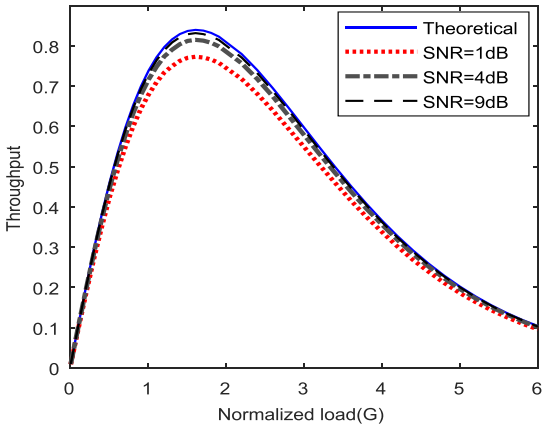

FIGURE 11. Normalized throughputs versus normalized load for PMSA with various SNR values.

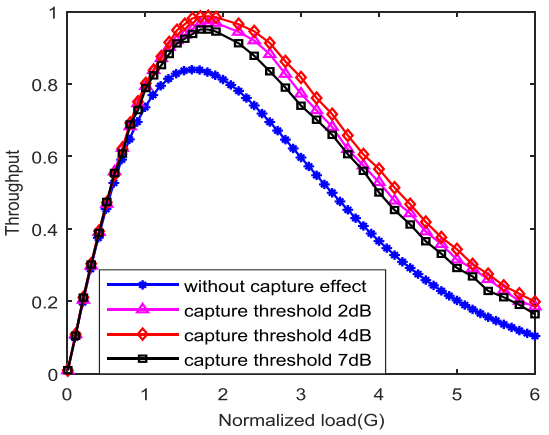

FIGURE 12. Normalized throughputs versus normalized load for PMSA with or without capture effect.

Fig.12 represents the throughput of the PMSA versus the normalized load for different thresholds of the capture effect. In the simulations, it is assumed that the power of users follows log-normally distribution with 0dB mean and standard deviation $\sigma = 3dB$. It can be seen that the throughputs of the PMSA with the capture thresholds are greater than that without the capture effect. The peak throughput with the threshold of 4dB approaches to 0.99, which is greater than that with the thresholds of 2dB and 7dB. The reason for this result is that, the compromise for the capture threshold of 4dB is better than that of 2dB and 7dB respectively.

VI. CONCLUSION

By using the polarized MIMO transmission signal model, we proposed a polarized MIMO slotted ALOHA (PMSA)

RA scheme. Without introducing the additional resource to transmit the packets more times, the collision of two packets can be effectively resolved by the MIMO detection algorithm in the PMSA, which increases the normalized throughput approaching 0.84. With the capture effect considered, some of the three overlapped packets may be decoded successfully, and the throughput approaches to 0.99 for the capture threshold of 4dB. Furthermore, the linearly polarized antennas have been considered in our study, and the same results will be achieved for the circularly polarized antennas. The focus point in the proposed scheme is the employment of the polarized MIMO transmission structure and detection algorithm to modify the SA, it can also be compatible with different CRDSA, IRSA schemes to further improve the throughput. Furthermore, the proposed PMSA is not only applied in the satellite network, but also can be used in the wireless network without the collision detection.

REFERENCES

[1] L. G. Roberts, "ALOHA packet systems with and without slots and capture," Telenet Commun. Corp., Washington, DC, USA, ARPANET Syst. Note 8 (NIC11290), Jun. 1972.

[2] N. Abramson, "The throughput of packet broadcasting channels," *IEEE Trans. Commun.*, vol. COM-25, no. 1, pp. 117–128, Jan. 1977.

[3] G. Choudhury and S. Rappaport, "Diversity ALOHA—A random access scheme for satellite communications," *IEEE Trans. Commun.*, vol. COM-31, no. 3, pp. 450–457, Mar. 1983.

[4] E. Casini, R. De Gaudenzi, and O. del Rio Herrero, "Contention resolution diversity slotted ALOHA (CRDSA): An enhanced random access scheme for satellite access packet networks," *IEEE Trans. Wireless Commun.*, vol. 6, no. 4, pp. 1408–1419, Apr. 2007.

[5] R. De Gaudenzi and O. D. Rio Herrero, "Advances in random access protocols for satellite networks," in *Proc. Int. Workshop Satellite Space Commun. (IWSSC)*, Sep. 2009, pp. 10–11.

[6] G. Liva, "Graph-based analysis and optimization of contention resolution diversity slotted ALOHA," *IEEE Trans. Commun.*, vol. 59, no. 2, pp. 477–487, Feb. 2011.

[7] M. Chiani, G. Liva, and E. Paolini, "The marriage between random access and codes on graphs: Coded slotted ALOHA," in *Proc. IEEE 1st AESS Eur. Conf. Satellite Telecommun. (ESTEL)*, Oct. 2012, pp. 1–6.

[8] S. E. El Ayoubi *et al.*, "Preliminary views and initial considerations on 5G RAN architecture and functional design," 5th Generat. Public Private Partnership, EURESCOM, METIS-II White Paper, Mar. 2016, pp. 1–27.

[9] X. Zhang and Z. Wang, "Characteristics of narrow band dual-polarized mimo over satellite channel model," in *Proc. Int. Conf. Comput. Commun. Netw. Technol. (ICCCNT)*, Jul. 2014, pp. 1–5.

[10] D. Benfatto, N. Privitera, R. Suffritti, A. Awoseyila, B. G. Evans, and S. Dimitrov, "On acquisition and tracking methods for SC-FDMA over satellite," in *Proc. 7th ASMS Conf./13th Signal Process. Space Commun. Workshops*, Sep. 2014, pp. 352–359.

[11] G. P. Yost and S. Panchapakesan, "Improvement in estimation of time of arrival (TOA) from timing advance (TA)," in *Proc. IEEE Int. Conf. Universal Pers. Commun.*, vol. 2. Oct. 1998, pp. 1367–1372.

[12] M. F. Pervej, M. Z. I. Sarkar, and M. T. Islam, "Impact analysis of different inputs and outputs block sizes of DFT-SCFDMA system," in *Proc. 2nd Int. Conf. Elect. Eng. Inf. Commun. Technol. (ICEEICT)*, May 2015, pp. 1–6.

[13] P. T. Mathiopoulos *et al.*, "Performance improvement techniques for the DVB-RCS2 return link air interface," *Int. J. Satellite Commun. Netw.*, vol. 33, no. 5, pp. 371–390, 2015.

[14] P. Haijiani and H. Shafiee, "Low complexity sphere decoding for space-frequency-coded MIMO-OFDM systems," in *Proc. 2nd IFIP Int. Conf. Wireless Opt. Commun. Netw.*, Mar. 2006, pp. 410–418.

[15] H. Noh, M. Kim, J. Ham, and C. Lee, "A practical MMSE-ML detector for a MIMO SC-FDMA system," *IEEE Commun. Lett.*, vol. 13, no. 2, pp. 902–904, Dec. 2009, doi: 10.1109/LCOMM.2009.12.091709.

[16] V. Almonacid and L. Franck, "Throughput performance of time- and frequency-asynchronous ALOHA," in *Proc. 11th Int. ITG Conf. Syst., Commun. Coding (SCC)*, Feb. 2017, pp. 1–6.

[17] C.-H. Chang and R. Y. Chang, "Design and analysis of multichannel slotted ALOHA for machine-to-machine communication," in *Proc. IEEE Global Commun. Conf. (GLOBECOM)*, Dec. 2015, pp. 1–6.

[18] J. Choi, "On the stability and throughput of compressive random access in MTC," in *Proc. IEEE Int. Conf. Commun. (ICC)*, Jul. 2017, pp. 1–6.

[19] J. Li, H. Tian, L. Xu, and Y. Huang, "An optimized random access algorithm for MTC users over wireless networks," in *Proc. IEEE 77th Veh. Technol. Conf. (VTC Spring)*, Jun. 2013, pp. 1–5.

[20] L. Kleinrock and S. Lam, "Packet switching in a multiaccess broadcast channel: Performance evaluation," *IEEE Trans. Commun.*, vol. COM-23, no. 4, pp. 410–423, Apr. 1975.

[21] A. Meloni and M. Murroni, "CRDSA, CRDSA++ and IRSA: Stability and performance evaluation," in *Proc. 12th Signal Process. Space Commun. Workshop (SPSC) 6th Adv. Satellite Multimedia Syst. Conf. (ASMS)*, Sep. 2012, pp. 220–225.

[22] S. Ghez, S. Verdu, and S. C. Schwartz, "Stability properties of slotted ALOHA with multipacket reception capability," *IEEE Trans. Autom. Control*, vol. AC-33, no. 7, pp. 640–649, Jul. 1988.

[23] M. Ghanbarinejad, C. Schlegel, and P. Gburzynski, "Adaptive probabilistic medium access in MPR-capable ad-hoc wireless networks," in *Proc. IEEE GLOBECOM*, Dec. 2009, pp. 1–5.

JIALING BAI was born in Shaanxi, China, in 1994. She received the B.S. degree in communications engineering from Xidian University, Xi'an, China, in 2016, where she is currently pursuing the M.S. degree in communication and information systems. Her research interests focus on the M2M satellite networks.

GUANGLIANG REN (M'06) was born in Jiangsu, China, in 1971. He received the B.S. degree in communications engineering from Xidian University, Xi'an, China, in 1993, the M.S. degree in signal processing from the Academy of China Ordnance, Beijing, China, in 1996, and the Ph.D. degree in communications and information systems from Xidian University in 2006. He is currently a Professor with the School of Telecommunications Engineering, Xidian University. He is the author of over 40 research papers in journals and conference proceedings, such as the IEEE TRANSACTIONS ON WIRELESS COMMUNICATIONS, the IEEE TRANSACTIONS ON COMMUNICATIONS, and the IEEE TRANSACTIONS ON VEHICULAR TECHNOLOGY and an author or co-author of three books. His research interests include wireless communications and digital signal processing, particularly multiple-input-multiple-output systems, WiMax, LTE, and so on.